17th World Conference on Earthquake Engineering, 17WCEE
Sendai, Japan - September 13th to 18th 2020
Paper N °C000339
Registration Code: S-A02095

SPECTRUM CHARACTERISTIC OF SOIL LAYERS AT SUBAO VILLAGE LANDSLIDE SITE

X. B. Li[(1)], X. Wang[(2)], C. Y. Chang[(3)]
[(1)] *Associate Professor, Institute of Disaster Prevention, xiaoboliiem@sina.cn*
[(2)] *Lecturer, Institute of Disaster Prevention, 344372776@qq.com*
[(3)] *Lecturer, Institute of Disaster Prevention, 991640583@qq.com*

Abstract

Seismic landslide is a common geological disaster, usually causing serious casualties and economic losses. The study of the spectrum features of typical landslide sites is crucial to better understanding the possible site response during earthquake, and then evaluate the risk of landslide. Therefore, we chose the Subao landslide to carry out microtremor survey and spectral analysis. Subao landslide located in Subao village, Xiji county, Ningxia Hui antonomous region, China, which was a giant coseismic loess landslide induced by 1920 Haiyuan great earthquake. The source area of the landslide had a length of about 1435 m, a width of about 400 m and an average thickness of about 30 m, with an irregular sliding surface. The scrap original height is about 153 m, a gentle terrain of 12 ° and apparent friction factor of 0.14, which was a typical low angle and long distance landslide.

To study the spectrum characteristics of Subao landslide site, we used a digital accelerograph to measure the microtremor on the sliding mass, landslide bed and soil mass of slopes around the landslide. The sampling rate is 200, and the data acquisition time is about 600 s. Then, based on the H/V method, applying the open source software Geopsy to calculate and analyze the test data. According to the results, we can draw the following conclusions: (1) Most H/V curves of soil mass of slopes around the landslide had clear peak, the range of the predominant frequency is 2.2 ~ 2.9 Hz, the peak amplification factor is 2.3 ~ 4.0, which were well reflected the magnification effect of ground motion about the soil mass and terrain; (2) H/V curves of the sliding mass were relatively gentle, multi-peak type, without significant predominant ranges, the peak amplification factor is 1.9 ~ 2.2, reflecting the complex interface of the soil after sliding and the no obvious amplification effect of the ground motion; (3) H/V curves at the outcrop of the landslide bed were had a narrow and steep predominant frequency band, the range of the predominant frequency is 2.4 ~ 2.6 Hz, the peak amplification factor is 4.6 ~ 4.8, showing significant topographic effect; (4) Compared with the stable soil mass of slopes around the landslide, the sliding mass was of complicated soil structure and the spectral characteristics were not obvious, therefore unable to well reflect the spectral features of the landslide site.

Accordingly, we found the spectral characteristics of soil mass of the slopes around the landslide are the reliable parameters for studying the dynamic stability of the landslide site. This would not only provide a criterion for the reasonable establishment of geomechanical models of slopes, but also provide the important calculation parameter for the inversion of ground motion based on coseismic landslide.

Keywords: Loess landslide, site, Spectrum characteristics; HVSR method; Dynamic stability

1. Introduction

Seismic landslide is a common earthquake-induced geological disaster that features “large scale, long sliding distance, gentle sliding surface, fragmented slip mass, heavy losses and high risk”. As early as the 780 BC, it had been documented that "all three areas of Jing, Wei, and Luo suffered an earthquake and dried up, causing the landslide of Qishan mountain." After entering the modern times, all major and great earthquakes (e.g., the 8.0-magnitude great earthquake in 1303 in Hongdong, Shanxi; the 7.5-magnitude major earthquake in 1718 in Tongwei, Gansu; the 8.5-magnitude great earthquake in 1920 in Haiyuan, Ningxia; and the 8.0-magnitude great earthquake in 2008 in Wenchuan, Sichuan) have caused very serious seismic landslides. The Haiyuan great earthquake (M = 8.5) in 1920 triggered 675 large scale loess landslides with a total area of 4,000 to 5,000 km^2. More than 100,000 people died for landslides buried villages and houses, which is account for about half of the earthquake’s death toll [1]. The Wenchuan great earthquake (M = 8.0) in 2008 triggered more than 35,000 landslides, which buried houses, destroyed buildings and blocked rivers, causing massive casualties and property losses [2,3]. Therefore, reducing the loss and risk of landslide disaster is one of the urgent problems in the field of seismic engineering.

How to reduce the loss and risk of earthquake landslide disaster? The primary task is to study the slope seismic stability and the landslide disaster mechanism. To study the slope seismic stability, we need to master the spectral characteristics of slope rock and soil mass, which is the key factor to ensure the reliability of research results. Analysis of the spectral characteristics of slope rock and soil mass is often based on microtremor test and horizontal-to-vertical spectral ratio (H/V) method. The microtremor is a continuous, non-repetitive, random fluctuation of the ground, referring to as inherent weak vibration on the earth's surface caused by natural forces such as meteorological, oceanic and geotectonic activities and human factors such as traffic [4]. Kanai and Tanaka [5] first used the microtremor records for estimating the site effect parameters. The H/V method proposed by Nakamura [6] has been widely applied to the site seismic response analysis. The H/V method is a kind of non-reference site method. The greatest advantage of H/V method is that it is not limited by the reference bedrock station during use. The H/V method is mainly based on the two aspects [6, 7]: (1) On the bedrock or hard soil layer, Fourier spectral ratio of horizontal component and vertical component of the vibration is approximate to 1; (2) The vertical component of the vibration is slightly affected by the local site conditions. In general, the H/V method can be used for estimating the site predominant frequency accurately, but the site amplification effect is underestimated [7, 8].

Lermo et al. [9] respectively used Fourier spectral ratio method, traditional spectral ratio method and spectral ratio method to carry out the spectral analysis based on the microtremor records on Acapulco, Oaxaca and Mexico City of Mexico. Through comparing the analysis result with that of the actual strong motion records, they argued that the site predominant period obtained by analyzing the microtremor records based on the H/V method is the most reasonable, and the site effect estimate based on the microtremor records is reliable. Seht and Wohlenberg [10] through analyzing the microtremor test data on the western site in the lower reaches of the Rhine Bay of Germany, argued that, compared with the traditional spectral ratio method, the H/V method has been proved that the better site predominant frequency can be obtained, its value is less affected by noise, and the correlation with the thickness of overlying soil layer is relatively good. Guo et al. [11] based on the 305 microtremor records on the bay area in the upper reaches of the Mississippi River, researched the site predominant period and the law of change in the mean shear wave velocity of soil layer using Nakamura spectral ratio method, and argued that, through the reliable estimate for the site predominant frequency based on the microtremor data, the changes in the relationship between the mean shear wave velocity of soil layer and the thickness of overlying soil layer can be conducted the inverse analysis. Soemitro et al. [12] based on the microtremor test data, analyzed the local site effect of the earthquake-induced landslide site using the H/V method, obtained site predominant frequency, amplification factor, vulnerability index and effective shear strain of the site soil layer, and carried out the initial assessment of dynamic stability of soil mass according to the range of change in value. Wang Wenpei et al. [13], taking Qingchuan Shiziliang slope in Wenchuan meizoseismal area as a typical example, according to the records on various elevations of aftershocks on the slopes and the microtremor test results, based on the simulation of dynamic stability of

slopes, discussed the impact of the slope forms on the spectrum signatures of slopes, and argued that the spectrum signatures of slopes were closely related to the slope form. Yin Yueping et al. [14], taking Qingchuan Donghekou seismic landslide in Wenchuan meizoseismal area as a typical example, according to the microtremor and numerical simulation results, researched the impact of the formation site effect on Donghekou seismic landslide, and argued that the damage caused by Donghekou landslide was triggered by the input seismic wave with high frequency spectrum value. Zare et al. [15], based on the microtremor test of landslide on the left side of Iran Latian reservoir dam, researched the site seismic response of landslides, and argued that dynamic properties of various locations on the landslide mass are significantly different, and the soil layer structure has a great effect on the site predominant frequency range of the soil mass. Aditya et al. [16] carried out the microtremor test in the high-risk area of landslide in Margoyosao village using the microtremor test technology, researched the spectrum signatures of soil mass in the potential landslide area, and determined the range of landslide-prone areas. Pappalardo et al. [17], based on geomorphologic and geophysical survey results, discussed the spectrum signatures of soil layer on the Abakainon cemetery site using H/V method, and drew a conclusion to build cemetery on the ancient landslide. Rezaei et al. [18] carried out the microtremor test of Nargeschal landslide in the southeast of Azad Shahr, Golestan, Iran, researched spectrum signatures, amplification effect, directional resonance effect, etc. of landslide soil mass, and argued that, by comparing with the actual survey result, the microtremor test is a reliable method for integrated assessment of landslide stability. Wang et al. [19], through the microtremor test and analysis of the landslide mass, verified the reliability of applying the microtremor test into internal structure detection of the landslide mass, whose research findings are of great significance for evaluation of landslide stability and research of instability mechanism. Hussain et al. [20], based on continuous microtremor observation data of Brazil Sobradinho landslide, researched the change laws of H/V curve and landslide soil properties (saturation, moisture content, consistency) using Nakamura spectral ratio method, and discussed the relationship between the spectrum signatures of landslide soil mass and the seasonal changes.

Above all, analyzing the site microtremor records using the H/V method can give the reliable predominant period of the site soil layer, and approximately estimate the site amplification effect, which is of great significance to the study of slope seismic stability. However, for seismic landslide, which part of the soil spectrum characteristics are most suitable for slope seismic stability analysis? This is still a question worth exploring. This paper takes the Ningxia Subao landslide as an example, carrying out microtremor test work, investigating the differences in the spectral characteristics of the non-sliding soil around the landslide, the landslide accumulation body and the laterite outcrocking at the back edge of the landslide, which provides the criterion for the reasonable construction of geomechanical model in the study of slope seismic stability and important calculation parameters for the inversion of ground motion based on seismic landslide.

2. Overview of landslide

Subao landslide is located in Subao village, Zhenhu Town, Xiji County, Ningxian Hui Autonomous Region (Fig. 1), within the IX seismic intensity area of Haiyuan mega-earthquake. The landslide is a low-angle long-runout landslide with an irregular plane (length nearly 1435m, width nearly 400m, average thickness nearly 30m, original slope height 153m, original slope 12 °, apparent friction factor 0.14). The landslide is located in the loess ridge area, where the strong seismic effect has led to the high-speed and long-runout slide of slope soil mass, so that the landslide mass has blocked the Hulu River and formed a dammed lake.

In order to better display the lithology of slope, and reflect structure characteristics of soil layer in the landslide area, the three drill holes were arranged on the landslide mass and the landslide boundary. The point locations and related information of the drill holes are shown in Fig. 2 and Table 1. ZK01 is located on the right wall of the landslide, ZK02 on the landslide deposit, and ZK03 on the left wall of the landslide. The drilling depth of each drill hole depends on the buried depth of Hipparion red soil (A red soil-like deposit dominated by lacustrine facies is widely distributed in Ningxia, Shaanxi and other provinces of China, whose lithology is dominated by hard clayed soil. Due to the richness of Hipparion fossil, such deposit is often called Hipparion red soil, and sometimes called mud rock or clay rock). The shear wave velocity test of soil

Fig. 1 – The Full View of Subao Landslide (Lens pointing, 165°)

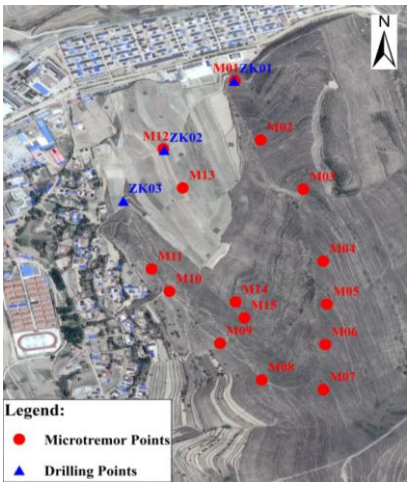

Fig. 2 – Drilling and Microtremor Points

Table 1 – Borehole Information

No.	Hole No.	Location	Depth (m)	Embedded depth of red clay (m)	Wave velocity test depth (m)	$V_{s,av}$ (m/s)	V_{se} (m/s)	Site class
1	ZK01	Right cliff	37	35.8	34	324	294	II
2	ZK02	Deposit	39.5	38	21	285	261	II
3	ZK03	Left cliff	10	8.8	8	185	182	—

layer uses single-hole method. Fig. 3 is a histogram of soil layers with the three drill holes. It can be seen that the lithology of soil layer in the landslide area is dominated by loess (alternation of silt and silty clay) and Hipparion red soil, and the loess is covered with the Hipparion red soil. ZK01～ZK03 are distributed in the northeast direction, and the thicknesses of loess layer are respectively 35.8m, 38m and 8.8m. Apparently, the landform of Hipparion red soil is shaped like a dustpan in the landslide area, high at the two sides and low in the middle, with good water holding capacity. Due to the limitation of test conditions, the depths of ZK01～ZK03 wave velocity test were respectively 35m, 21m and 8m, and the mean shear wave velocities were, in turn, 324m/s, 285m/s and 185m/s. Moreover, according to Code for Seismic Design of Buildings (GB 50011-2010) (2016 Version), ZK01～ZK03 respectively have the mean shear wave velocities of 294m/s, 261m/s and 182m/s, being the class-II sites.

3. Acquisition and processing of data

In order to discuss the differences between the spectrum signatures of soil masses in the landslide area, the digital strong-motion seismograph is used in carrying out the microtremor test of the unslided soil mass around the landslide, landslide deposit and exposed red soil on the rear edge of landslide. The locations of measuring points are shown in Fig. 2. M01～M11 are located on the unslided soil mass and distributed along the landslide boundary, whose specific locations are determined by geographic and geomorphic conditions; M12 and M13 are located on the landslide deposit, and distributed along main sliding direction of landslide; M14 and M15 are located on exposed Hipparion red soil on the rear edge of landslide. In order to improve the accuracy of microtremor data, the site leveling prior to data acquisition can ensure that the instruments are in good contact with the ground, and arranged in the three directions: North-South (NS), West-East (EW) and Upright Direction (UD) to obtain the microtremor data. According to SESAME Guidelines and Code for Measurement Method of Dynamic Properties of Subsoil, the test is generally conducted in a relatively quiet external environment, with the sampling rate of 200, and the data acquisition time of 600 s.

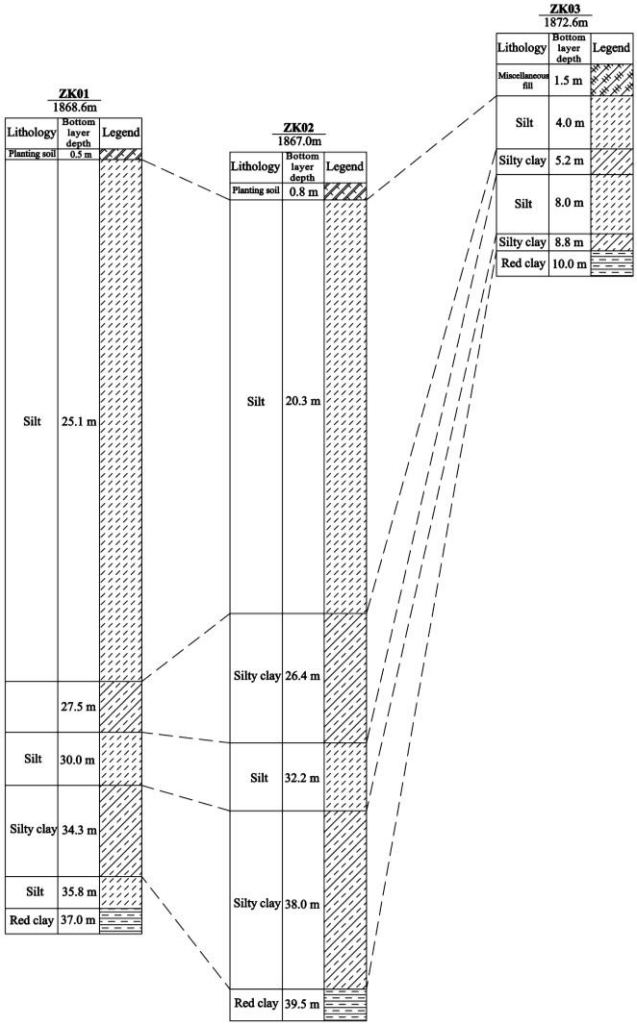

Fig. 3 Histogram of Soil Layers with ZK01～ZK03

After the data acquisition, based on H/V method, the open-source software Geopsy is used to process and analyze the microtremor data. The processing steps of microtremor data mainly include data selection, band-pass filtering, calculating of Fourier spectrum, smoothing and calculation of H/V value [8]. (1) Data selection: The duration of data window is set as 20 s; the microtremor data are acquired from the three directions (NS, EW and UD); in order to ensure the stability of signal in the data window, the data from the three directions in each time window must meet the criteria of $0.5 < \text{STA/LTA} < 2.0$, the long-short time ratios of data in this paper are STA = 1.0 s, and LTA = 30.0 s; the data in the time window are allowed 20% overlap. (2) Band-pass filtering: In order to ensure the reliability of analysis result, the fourth-order Butterworth band-pass filtering function is used for the filtering processing of primary microtremor data; the filtering bandwidth is 0.05 ～ 20.00 Hz; the filtered data are tested again under the condition of $0.5 < \text{STA/LTA} < 2.0$; (3) Calculation of Fourier spectrum: After the filtering processing is completed, the data in each data time window are carried out Fast Fourier Transform (FFT) to obtain Fourier spectral value from the three directions (NS, EW and UD), thereby completing the conversion of microtremor data from time domain to frequency domain; (4) Smoothing: The data in each Fourier spectrum window are carried out smoothing using Konno-Ohmachi function [21, 22], and the bandwidth factor b is 40; (5) Calculation of H/V value: The H/V value of each Fourier spectrum window is calculated separately using the H/V method to obtain an H/V curve, in which the values in the horizontal direction (H direction) are taken from the mean square value in the NS and EW directions, and the value of the H/V curve of each measuring point is taken from the mean

value of the H/V curves of Fourier spectrum windows. More information on the data analysis and processing can be seen from SESAME Guidelines.

The shape of H/V curve is related to the site conditions, including various types, such as uni-peak type, bi-peak type and multi-peak type. Various types of H/V curves have various peak frequencies f_0 and peak amplification factors A_0. The determination of typical peak frequency f_0 and peak amplification factor A_0 at the measuring points is based on 5 conditions [8]: (1) $A_0 > 2$; (2) Within the range of $[f_0/4, f_0]$ frequency, there exists at least an H/V value ($A_{H/V}$) which is less than $A_0/2$; (3) Within the range of $[f_0, 4f_0]$ frequency, there exists at least an H/V value ($A_{H/V}$) which is less than $A_0/2$; (4) Within the range of the peak frequency f_0, the standard deviation σ_f of the peak frequency f_0 shall be less than the threshold value $\varepsilon(f_0)$ specified in Table 2; (5) Within the range of the peak frequency f_0, the standard deviation σ_A of the peak amplification factor A_0 shall also be less than the threshold value $\theta(f_0)$ specified in Table 2. Generally speaking, if the H/V curve of a measuring point can meet 4 of the above 5 conditions, f_0 can be used for the reliable estimate for the site predominant frequency f_d of soil layer at this point.

Table 2 – Threshold Values for Stability Conditions [8]

Frequency range (Hz)	＜0.2	0.2～0.5	0.5～1.0	1.0～2.0	＞2.0
$\varepsilon(f_0)$ (Hz)	0.25 f_0	0.20 f_0	0.15 f_0	0.10 f_0	0.05 f_0
$\theta(f_0)$	3.0	2.5	2.0	1.78	1.58

4. Results

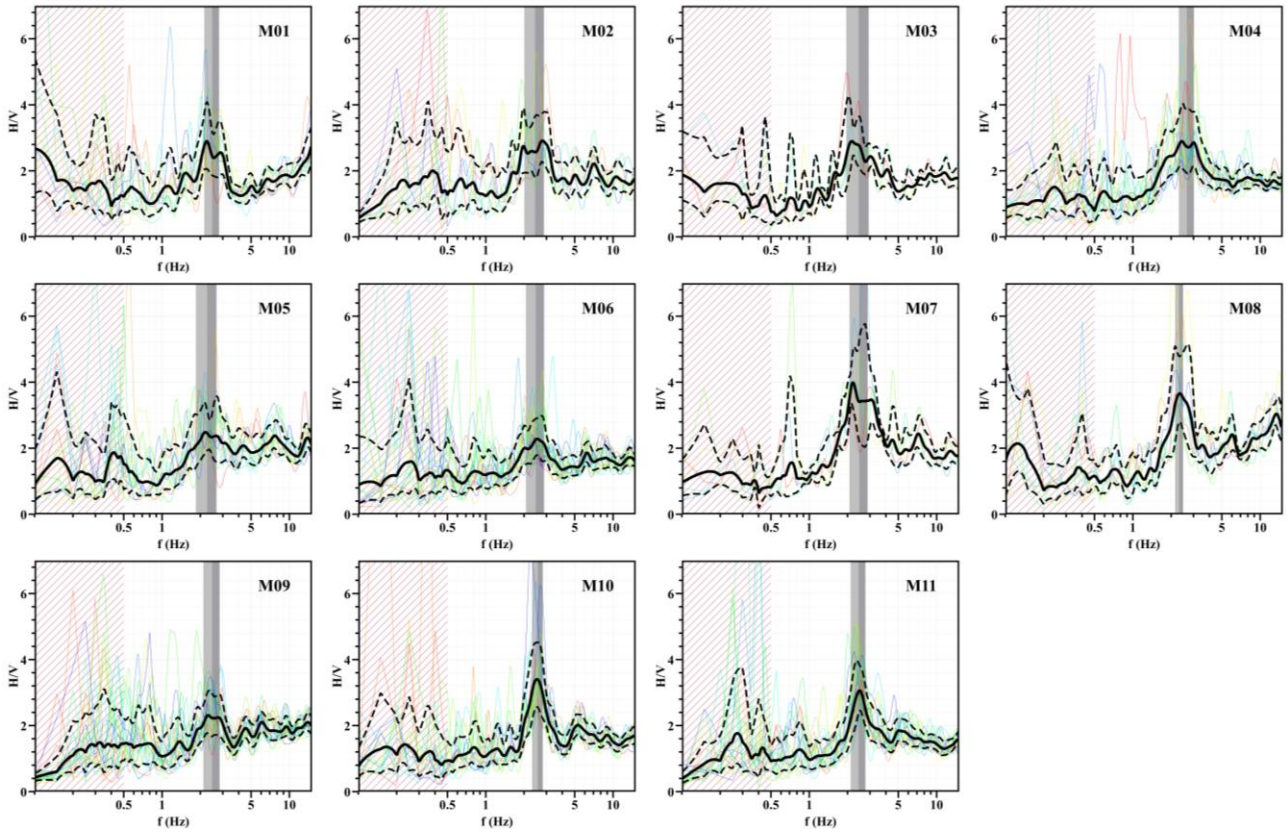

Fig. 4 H/V Curves of Measuring Points M01～M11

The range of frequency is 0.1 ～ 15 Hz; the colored lines represent the H/V curves of various Fourier spectrum windows at various points, the black solid lines represent the mean values of various H/V curves, and the black dotted lines represent the mean H/V curve multiplied/divided by one time standard deviation σ_A; the grey bars represent the mean values of peak frequencies f_0 of H/V curves of various Fourier spectrum windows plus/minus one time standard deviation σ_f, and the pink area represents unreliable frequency band; the same below.

The H/V curves of M01～M11 on the unslided soil mass around the landslide are shown in Fig. 4. It can be seen from Fig. 4 that the H/V curves of M01～M11 are dominated by the uni-peak type, and have relatively obvious peak frequency bands. Table 3 lists peak frequency f_0 and peak amplification factor A_0 of mean H/V curves of M01～M11, in which 2.2 Hz ≤ f_0 ≤ 2.8 Hz, 2.3 ≤ A_0 ≤ 4.0 indicate the characteristic of the peak frequencies at various points, which are dominated by high frequency and have relatively obvious amplification effect. According to the conditions for the reliable estimate for the site predominant frequency f_d of soil layer, the peak frequencies f_0 of M01, M03, M07, M08, M10 and M11 can be used for the reliable estimate for the site predominant frequency f_d of soil layer (Table 3). Therefore, the range of the site predominant frequency of unslided soil mass around the landslide is 2.2 Hz ≤ f_d ≤ 2.6 Hz, and the range of the corresponding peak amplification factor is 2.9 ≤ A_0 ≤ 4.0.

Table 3 – The f_0, A_0 Value of Points M01～M15 and The Reliable Estimation of f_d

Points No.	**Location**	**f_0 (Hz)**	**A_0**	**The reliable estimation of f_d**					
				A_0>2	**There exists one frequency f lying $[f_0/4, f_0]$, such that $A_{H/V} < A_0/2$**	**There exists one frequency f lying $[f_0, 4f_0]$, such that $A_{H/V} < A_0/2$**	$\sigma_f < \varepsilon(f_0)$	$\sigma_A < \theta(f_0)$	**Result**
M01	Right cliff	2.3	2.9	Y	Y	Y	N	Y	**Y**
M02		2.8	2.9	Y	Y	N	N	Y	N
M03		2.2	2.9	Y	Y	Y	N	Y	**Y**
M04		2.4	2.9	Y	Y	N	N	Y	N
M05		2.2	2.5	Y	Y	N	N	Y	N
M06		2.6	2.3	Y	Y	N	N	Y	N
M07	Top	2.2	4.0	Y	Y	Y	N	Y	**Y**
M08	Left cliff	2.3	3.7	Y	Y	Y	N	Y	**Y**
M09		2.3	2.3	Y	Y	N	N	Y	N
M10		2.6	3.4	Y	Y	Y	N	Y	**Y**
M11		2.5	3.1	Y	Y	Y	N	Y	**Y**
M12	Deposit	8.0	1.9	N	N	N	N	Y	N
M13		13.0	2.2	Y	Y	N	N	Y	N
M14	Landslide bed	2.6	4.6	Y	Y	Y	N	Y	Y
M15		2.4	4.8	Y	Y	Y	N	Y	Y

The H/V curves of M12 and M13 on the landslide deposit are shown in Fig. 5. It can be seen that the H/V curves of M12 and M13 change gently, and belong to the multi-peak type, without any obvious peak frequency band; and the amplification effect is not significant, and the peak amplification factor changes

around 2. The statistical results in Table 3 indicate that the results of M12 and M13 could not be used for the reliable estimate for the site predominant frequency of deposit.

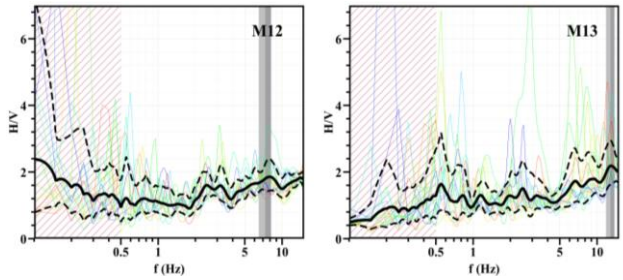

Fig. 5 H/V Curves of Measuring Points M12～M13

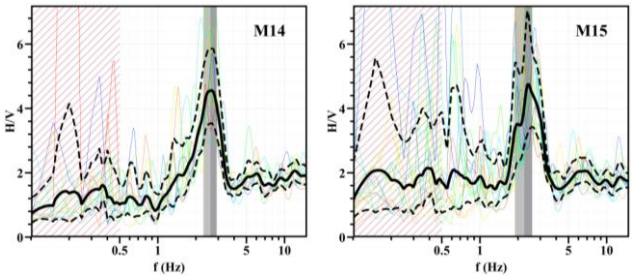

Fig. 6 H/V Curves of Measuring Points M14～M15

The H/V curves of M14 and M15 on the exposed Hipparion red soil on the rear edge of landslide are shown in Fig. 6. It can be seen that the H/V curves at the two measuring points belong to typical uni-peak type, with obvious peak frequency band and significant amplification effect. According to Table 3, the peak frequencies of M14 and M15 are respectively 2.6 Hz and 2.4 Hz, the peak amplification factors are respectively 4.6 and 4.8, and the consistent results are conducive to make a reliable estimate for the site predominant frequency of Hipparion red soil on the rear edge of landslide. Therefore, the site predominant frequency range of Hipparion red soil in Subao landslide area is 2.4 Hz $\leq f_d \leq$ 2.6 Hz, and the range of the corresponding peak amplification factor is $4.6 \leq A_0 \leq 4.8$.

5. Discussion and Conclusion

The loess is a kind of typical Quaternary loose deposit, which is often deposited by wind transportation, without stratification. Deposit thickness and landform of the loess are mainly controlled by underlying primary landform. If the primary landform is different, the thickness of overlying loess is different. The histogram of drill holes of ZK01～ZK03 (Fig. 3) indicates that the primary landform in Subao landslide area is shaped like a dustpan, high at the two sides and low in the middle, but higher on the left side than on the right side. The change of landform directly leads to the difference in the deposit thickness of overlying loess, for example, although the soil layer structure of ZK03 on the left side of landside is generally consistent with those of ZK01 and ZK02, the thicknesses of various soil layers are quite different. The impact of primary landform and thickness of overlying soil layer on the spectrum signatures of the site soil layer can be reflected in the H/V curves of various microtremor measuring points.

For the measuring points on the unslided soil mass around the landslide, the peak frequencies of M01, M03, M07, M08, M10 and M11 can be used for the reliable estimate for the site predominant frequency of soil layer. Although their peak frequencies only have little difference, compared with the measuring points on the right wall (M01, M03), the H/V curves of the measuring points on the left wall (M08, M10, M11) have narrow predominant frequency band and high amplification factor, which reflect the characteristics of relatively thin overlaying soil layer, relatively narrow buried depth of abrupt interface of shear wave velocity. It is similar to the formation conditions revealed by the drill holes ZK01 and ZK03 in Fig. 3. The thickness h of the overlying soil layer can be determined according to the empirical formula $h_{\min} \approx V_{s,av}/4f_0$. For example, ZK01 and M01 are located at the same location. According to the measured mean shear wave velocity $V_{s,av}$ = 324 m/s, f_0 = 2.3 Hz, the lower limit depth of overlying soil layer $h_{\min} \approx$ 35.2 m can be obtained, which is only 0.6m different from the buried depth of red soil of ZK01 in Table 1, so that the thickness of overlying soil layer can be estimated better. Although the H/V method underestimates the site amplification effect, the peak amplification factor of M07 at the top of the rear edge of landslide is higher than that on the left and right walls. The peak amplification factor is also affected by the height of landform. Therefore, the microtremor test results of the unslided soil mass can better reflect the site predominant frequency of the site

soil layer, but the estimation of the site amplification effect is also affected by the specific location of the measuring points.

Compared with the measuring points on the unslided soil mass around the landslide, the H/V curves of the measuring points M12 and M13 on the landslide deposit change gently, without any obvious peak frequency band, and the amplification effect is not significant. Under the action of the seismic ground motion, the slope soil mass as a whole slides downwards. Original characteristic of downslope deposit under the action of the wind transportation no longer exists. In the landslide deposit, although the sequence of soil layer has not changed significantly (ZK02 in Fig. 3), the unconformable contact relationship between the deposit and the primary landform has led to the change in the wave propagation path without any obvious directionality, which shall be the main reason that the H/V curve appears as the multi-peak type. In addition, the phenomena during the drilling process, such as serious water leakage and sampling difficulty, reflect looseness of the deposit soil layer and fracture development, which have a certain absorption effect on the wave propagation, thereby resulting in the unremarkable amplification effect of soil layer. Compared with the unslided soil mass, the spectrum signatures of the measuring points on the deposit can not really reflect those of soil layer on the slope site; therefore, they shall not be used for the reliable estimate for spectrum signatures of soil layer on the slope site.

For M14 and M15 on the rear edge of landslide, due to the exposure of Hipparion red soil at the measuring points, without overlaying loess layer, the interfacial wave velocity changes greatly, and the amplification effect of the two points is significant, and the peak amplification factor is up to 4.6 ～ 4.8. The stratigraphic characteristics of loess indicate that the underlying Hipparion red soil of loess is often severely weathered on the surface, the shear wave velocity is significantly different from deeply unweathered bedrock wave velocity, and the wave impedance effect is obvious, which can be reflected when the predominant frequency bands of M14 and M15 are under the high frequency band. However, due to the lack of measured shear wave velocity data, it is not possible to make a reliable estimate for the buried depth of deeply unweathered bedrock surface.

Above all, through processing and analysis of the microtremor test data of soil layer in the Subao landslide area, we argued that the microtremor test results of the unslided soil mass around the landslide, landslide deposit and exposed Hipparion red soil on the rear edge of landslide can better reflect the structure characteristics of the site soil layer. Compared with the landslide deposit, the spectrum signatures of the measuring points on the unslided soil mass and the exposed red soil on the rear edge of landslide are more obvious, and the acquired peak frequency band can be used for the reliable estimate for predominant frequency band of the site soil layer. Due to the limitation of H/V method, the actual amplification effect of the peak amplification factor is underestimated. It is suggested to use the H/V method cautiously. The conclusion of this paper is drawn based on the Subao landslide; therefore, its limitation is inevitable. However, it is also valuable as an exploration. Therefore, this paper argues that the spectrum signatures of the unslided soil mass around the landslide are reliable parameters to research the dynamic stability of landslide site, which not only can provide the criteria for the rational constructions of geomechanical models of slopes, and but also can provide important calculating parameters for the reverse seismic ground motion based on the seismic landslide.

6. References

[1] Lanzhou Institute of Seismology, CEA, Ningxia Hui Autonomous Region Earthquake Team (1980): *1920 Haiyuan great earthquake*. Beijing: Seismological Press.

[2] Huang R Q, Li W L (2008): Research on development and distribution rules of geohazards induced by Wenchuan earthquake on 12th May. *Chinese Journal of Rock Mechanics and Engineering*, **27**(12), 2587-2592.

[3] Yin Y P (2009). Rapid and long run-out features of landslides triggered by the Wenchuan earthquake. *Journal of Engineering Geology*, **17**(2), 153-166.

[4] Ministry of Housing and Urban-Rural Development of the People's Republic of China, General Administration of Quality Supervision, Inspection and Quarantine of the People's Republic of China (2015). *Code of measurement methods of dynamic properties of subsoil* (GB/T 50269-2015). Beijing: China planning press.

[5] Kanai K., Tanaka T (1954). Measurement of the microtremor I. *Bulletin of the Earthquake Research Institute of Tokyo University*, **32**, 199-209.

[6] Nakamura Y (1989). A method for dynamic characteristics estimation of subsurface using microtremor o the ground surface. *Q. Rep. Railw. Tech. Res. Inst*., **30**, 25-33.

[7] Rezaei S, Choobbasti A. J (2017). Application of the microtremor measurements to a site effect study. *Earthquake Science*, **30**(3), 157-164.

[8] Bard P.-Y., SESAME-Team (2004). Guidelines for the Implementation of the H/V Spectral Ratio Technique on Ambient Vibrations-Measurements, Processing and Interpretations. *SESAME European Research Project EVG1-CT-2000-00026*, D23.12.

[9] Lermo J, Chavez-Garcia J F (1994). Are Microtremors Useful in Site Response Evaluation? *Bulletin of the Seismological Society of America*, **84**(5), 1350-1364.

[10] Seht I M, Wohlenberg J (1999). Microtremor Measurements Used to Map Thickness of Soft Sediments. *Bulletin of the Seismological Society of America*, **89**(1), 250-259.

[11] Guo Z, Aydin A, Kuszmaul J S (2014). Microtremor recording in Northern Mississippi. *Engineering Geology*, **179**, 146-157.

[12] Soemitro R A, Warnana D D, Utama W, Asmaranto R (2011). Assessment to the Local Site Effects during Earthquake Induced Landslide Using Microtremor Measurement (Case Study Kemuning Lor, Jember Regency-Indonesia). *J. Basic. Appl. Sci. Res.*, **1**(5), 412-417.

[13] Wang W P, Yin Y P, Li B, Feng Z, Yan J K (2015). Spectral characteristics of dynamic response of slope with different angles of inclination. *Chinese Journal of Rock Mechanics and Engineering*, **34**(1), 121-128.

[14] Yin Y P, Wang W P, Li B, Zhang N, Li H T (2016). Study of stratigraphic site effect on the failure mechanism of Donghekou rockslide triggered by Wenchuan earthquake. *China Civil Engineering Journal*, **49**(S2), 126-131.

[15] Zare M A, Haghshenas E, Jafari M K (2017). Interpretation of dynamic response of a very complex landslide (Latian-Tehran) based on ambient noise investigation. *Soil Dynamics and Earthquake Engineering*, **100**, 559-572.

[16] Aditya M R, Romadlon A F, Medika R A, Alfontius Y, Jannet Z D, Hartantyo E (2018). Zonation of Landslide-Prone Using Microseismic Method and Slope Analysis in Margoyoso, Magelang. *Journal of Physics: Conf. Series*, **1011**.

[17] Pappalardo G, Imposa S, Barbano M S, Grassi S, Mineo S (2018). Study of landslides at the archaeological site of Abakainon necropolis (NE Sicily) by geomorphological and geophysical investigations. *Landslides*, **15**, 1279-1297.

[18] Rezaei S, Shooshpasha I Rezaei H (2018). Empirical Correlation between Geotechnical and Geophysical Parameters in a Landslide Zone (Case Study Nargeschal Landslide). *Earth Sci. Res. J.*, **22**(3), 195-204.

[19] Wang F W, Okeke A C, Kogure T, Sakai T, Hayashi H (2018). Assessing the Internal Structure of Landslide Dams subject to Possible Piping Erosion by means of MTM Chain Array and SP Surveys. *Engineering Geology*, **234**, 11-26.

[20] Hussain, Y., Martinez-Carvajal, H., Condori, C., Uagoda, R., Cárdenas-Soto, M., Cavalcante, A. L. B., Cunha, L. S. da, Martino, S (2019). Ambient Seismic Noise: a continuous source for the dynamic monitoring of landslides. *Terræ Didatica*, **15**, 1-5.

[21] Konno K, Ohmachi T (1998). Ground-Motion Characteristics Estimated from Spectral Ratio between Horizontal and Vertical Components of Microtremor. *Bulletin of the Seismological Society of America*, **88**(1), 228-241.

[22] Rodriguez V H S, Midorikawa S (2002). Applicability of the H/V spectral ratio of microtremors in assessing site effects on seismic motion. *Earthquake Engng Struct. Dyn.*, **31**, 261-279.

